# Phase-controlled optical switching and slow- and weak-light solitons in a coherent molecular system with permanent dipole moments

**Qiong Du, Chao Hang, and Guoxiang Huang***

*State Key Laboratory of Precision Spectroscopy and Department of Physics, East China Normal University, Shanghai 200062, China*
**Corresponding author: gxhuang@phy.ecnu.edu.cn*

Received September 23, 2013; revised December 4, 2013; accepted January 10, 2014; posted January 27, 2014 (Doc. ID 197896); published February 26, 2014

We investigate the linear and nonlinear light pulse propagations in a three-level Λ-type molecular system with permanent dipole moments via electromagnetically induced transparency (EIT). We find that EIT characters in such a system depend strongly on the phase of control field, based on which a phase-controlled optical switch can be designed. We show that the Kerr nonlinearity of the system can be largely enhanced due to the control-field-induced quantum interference effect. We derive a nonlinear Schrödinger equation for the evolution of the probe-field envelope and demonstrate that it is possible to generate stable slow- and weak-light solitons in the system. © 2014 Optical Society of America

*OCIS codes:* (020.1670) Coherent optical effects; (270.5530) Pulse propagation and temporal solitons.
http://dx.doi.org/10.1364/JOSAB.31.000594

## 1. INTRODUCTION

Laser-induced interference plays an important role in interactions of light and matter, and has found numerous applications in atomic, molecular, and optical physics. One such example is electromagnetically induced transparency (EIT) [1]. By means of the quantum interference effect induced by a control field, the absorption of a probe field can be largely suppressed, and hence an initially highly opaque optical medium can become transparent. EIT is a very typical quantum interference phenomenon, which can be used to manipulate physical properties for both light and matter, including large reduction of group velocity [2,3] and giant enhancement of Kerr nonlinearity [4,5]. Based on these important features, EIT has been used to realize slow light, quantum memory [6,7], highly efficient four-wave mixing [8], high-precision measurement [9], quantum phase gates [10,11], weak-light ultraslow solitons [12–15], spatial solitons [16–20], and so on.

Although most studies on EIT are focused on atomic systems, in recent years there has been much investigation of EIT in molecular systems both theoretically and experimentally [21–31]. However, up to now less attention has been paid to the EIT in molecules with permanent dipole moments (PDMs). A dipolar molecule with PDM is the one with states having no parity symmetry and having a nonvanishing difference between diagonal dipole matrix elements. In recent years, it has been shown that PDMs can significantly modify the resonant couplings between laser field and molecules and allow some new optical transitions to occur [32,33].

In a recent work, Zhou *et al.* [34] investigated the EIT in a three-level Λ-type molecular system with PDMs. For a $(1+1)$-transition processes, it was found that there are not significant differences for EIT between systems with and without PDMs. Later, Ma *et al.* [35] considered the EIT in a three-level ladder-type molecular system with PDMs. Some additional PDM-induced coherent optical effects (e.g., gain without inversion and fast light) are also predicted in Refs. [34,35].

In this article, we investigate the linear and nonlinear light pulse propagations in a three-level Λ-type molecular system with PDMs via EIT. We find that the EIT character for $(1+1)$-transition processes depends strongly on the phase of control field, based on which a phase-controlled optical switch can be devised. We show that the Kerr nonlinearity of the system can be largely enhanced due to the control-field-induced quantum interference effect. We derive a nonlinear Schrödinger (NLS) equation for the evolution of the probe-field envelope and demonstrate that it is possible to create stable slow- and weak-light solitons in the system.

The rest of the article is arranged as follows. In Section 2, the physical model of the three-level Λ-type molecular system with PDMs is described, and the solution in the linear regime is presented. In Section 3, the phase-dependent EIT property is discussed and the phase-controlled optical switching is constructed. In Section 4, the NLS equation is derived using a method of multiple scales, and stable slow- and weak-light solitons are demonstrated based on the Kerr nonlinearity enhancement of the system. The last section contains a summary of our main results.

## 2. MODEL AND SOLUTION IN LINEAR REGIME

We consider a system consisting of $N_m$ noninteracting polar molecules with a Λ-type level configuration. The molecules interact with a strong, continuous-wave control field of angular frequency $\omega_c$ driving the transition $|2\rangle \leftrightarrow |3\rangle$, and a weak, pulsed probe field (with pulse length $\tau_0$ and beam radius $R_\perp$ at the entrance of the medium) of center angular frequency

 

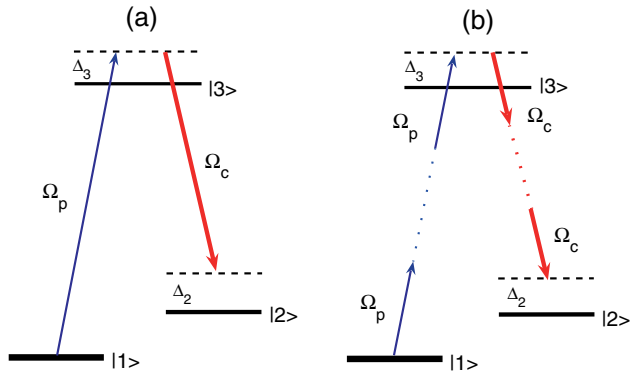


Fig. 1. Energy-level diagram and excitation scheme of the three-level Λ-type polar molecular system. A weak (strong) probe (control) field of central angular frequency $\omega_p$ ($\omega_c$) and Rabi frequency $\Omega_p$ ($\Omega_c$) couples to the atomic states $|1\rangle$ ($|2\rangle$) and $|3\rangle$. (a) $(1+1)$-transition process. (b) $(m+n)$ transition process $(m,n=2,3,4,\ldots)$.

$\omega_p$ driving the transition $|1\rangle\leftrightarrow|3\rangle$, respectively (Fig. 1). In the $(1+1)$-transition process, the transition $|1\rangle\leftrightarrow|3\rangle$ ($|2\rangle\leftrightarrow|3\rangle$) is driven by one probe (control) photon, satisfying the resonant condition $E_3-E_1\approx\hbar\omega_p$ ($E_3-E_2\approx\hbar\omega_c$), with $E_j$ being the eigenenergy of the state $|j\rangle$ [Fig. 1(a)]. Generally, the system also allows the $(m+n)$-transition process $(m,n=1,2,3,\ldots)$ [34], where the transition $|1\rangle\leftrightarrow|3\rangle$ ($|2\rangle\leftrightarrow|3\rangle$) is driven by $m$ probe ($n$ control) photons [Fig. 1(b)], satisfying the resonant condition $E_3-E_1\approx m\hbar\omega_p$ ($E_3-E_2\approx n\hbar\omega_c$). In this work, for simplicity we consider only the $(1+1)$-transition process. The case of the $(m+n)$-transition process will be considered elsewhere. In addition, each laser field contains a large amount of photons, and hence they can both be considered as classical fields.

The Hamiltonian of the system is given by $\hat{H}=\hat{H}_0+\hat{H}'$, where $\hat{H}_0$ and $\hat{H}'$ describe a free molecule and the interaction between the molecule and a laser field, respectively. In the Schrödinger picture, the state vector of the system is $|\Psi(\mathbf{r},t)\rangle=\sum_{j=1}^{3}C_j(\mathbf{r},t)|j\rangle$, where $|j\rangle$ is the eigenvector of $\hat{H}_0$ with the eigenenergy $E_j$, i.e., $\hat{H}_0|j\rangle=E_j|j\rangle$, and $C_j$ is the probability amplitude of the state $|j\rangle$. Under electric-dipole approximation, the Hamiltonian of the system reads

$$H=\sum_{j=1}^{3}(E_j-\mathbf{p}_{jj}\cdot\mathbf{E})|j\rangle\langle j|-(\mathbf{p}_{31}\cdot\mathbf{E}|3\rangle\langle 1|+\mathbf{p}_{32}\cdot\mathbf{E}|3\rangle\langle 2|+\text{H.c.}), \tag{1}$$

where $\mathbf{p}_{ij}$ is the electric-dipole matrix element associated with the transition from $|j\rangle$ to $|i\rangle$; $\mathbf{E}(\mathbf{r},t)=\sum_{\alpha=c,p}\mathbf{e}_\alpha\mathcal{E}_\alpha e^{i(\mathbf{k}_\alpha\cdot\mathbf{r}-\omega_\alpha t)}+$ c.c. is the expression of the laser field, with $\mathbf{k}_p$, $\mathbf{e}_p$, $\mathcal{E}_p$ ($\mathbf{k}_c$, $\mathbf{e}_c$, $\mathcal{E}_c$) being the wavevector, unit polarization vector, and envelope of the probe (control) field, respectively; and H.c. denotes the corresponding Hermitian conjugate term. Notice that due to the existence of PDMs, $\mathbf{p}_{jj}$ $(j=1,2,3)$ are nonzero in the present system.

In order to investigate the time evolution of the system, it is more convenient to employ an interaction picture, which is obtained by making the transformation $C_j(\mathbf{r},t)=A_j(\mathbf{r},t)\exp[i(\mathbf{k}_j\cdot\mathbf{r}-\omega_j t-\Delta_j t)+(i/\hbar)\mathbf{p}_{jj}\cdot\int\mathrm{d}t'\mathbf{E}(\mathbf{r},t')]$, with $\mathbf{k}_1=0$, $\mathbf{k}_2=\mathbf{k}_p-\mathbf{k}_c$, $\mathbf{k}_3=\mathbf{k}_p$, $\Delta_1=0$, $\Delta_3=\omega_p-(\omega_3-\omega_1)$ (one-photon detuning), and $\Delta_2=\omega_p-\omega_c-(\omega_2-\omega_1)$ (two-photon detuning). Substituting the laser field, which can be further expressed as $\mathbf{E}(\mathbf{r},t)=2\sum_{\alpha=c,p}\mathbf{e}_\alpha[\mathrm{Re}(\varepsilon_\alpha)\cos\theta_\alpha-\mathrm{Im}(\varepsilon_\alpha)\sin\theta_\alpha]$ with $\theta_\alpha=\mathbf{k}_\alpha\cdot\mathbf{r}-\omega_\alpha t$, into the transformation, the exponential function including the integral can be expressed as

$$\begin{aligned}e^{\frac{i}{\hbar}(\mathbf{p}_{ll}-\mathbf{p}_{jj})\cdot\int^t\mathrm{d}t'\mathbf{E}(\mathbf{r},t')}&=e^{iP_{jl}^p\sin\theta_p+iQ_{jl}^p\cos\theta_p+iP_{jl}^c\sin\theta_c+iQ_{jl}^c\cos\theta_c}\\&=\sum_{m=-\infty}^{\infty}J_m(P_{jl}^p)e^{im\theta_p}\sum_{n=-\infty}^{\infty}J_n(Q_{jl}^p)e^{in\left(\frac{\pi}{2}-\theta_p\right)}\\&\quad\times\sum_{\mu=-\infty}^{\infty}J_\mu(P_{jl}^c)e^{i\mu\theta_c}\sum_{\nu=-\infty}^{\infty}J_\nu(Q_{jl}^c)e^{i\nu\left(\frac{\pi}{2}-\theta_c\right)},\end{aligned}$$

where $m,n,\mu,\nu=0,1,2,\ldots$, $P_{jl}^\alpha=-2(\mathbf{e}_\alpha\cdot(\mathbf{p}_{jj}-\mathbf{p}_{ll})/\hbar\omega_\alpha)\,\mathrm{Re}(\varepsilon_\alpha)$, and $Q_{jl}^\alpha=-2(\mathbf{e}_\alpha\cdot(\mathbf{p}_{jj}-\mathbf{p}_{ll})/\hbar\omega_\alpha)\,\mathrm{Im}(\varepsilon_\alpha)$. $J_m$ is the $m$-order Bessel function, and we have used the relation $e^{iz\sin x}=\sum_{m=-\infty}^{\infty}J_m(z)e^{imx}$.

We focus on the $(1+1)$-transition process. To this end, we take $m=n=\mu=\nu=0$. Under the rotating-wave approximation, it is easy to obtain the Hamiltonian in the interaction picture

$$H_{\text{int}}=\hbar[\Delta_2|2\rangle\langle 2|+\Delta_3|3\rangle\langle 3|+\rho_1\Omega_p|3\rangle\langle 1|+\rho_2\Omega_c|3\rangle\langle 2|+\text{H.c.}], \tag{2}$$

where $\Omega_p=\mathbf{e}_p\cdot\mathbf{p}_{31}\mathcal{E}_p/\hbar$ and $\Omega_c=\mathbf{e}_c\cdot\mathbf{p}_{32}\mathcal{E}_c/\hbar$ are, respectively, the Rabi frequencies of the probe and control fields, and $\rho_1$ and $\rho_2$ are given by

$$\rho_1=J_0(P_{31}^c)J_0(Q_{31}^c)J_0(P_{31}^p)J_0(Q_{31}^p), \tag{3a}$$

$$\rho_2=J_0(P_{32}^c)J_0(Q_{32}^c)J_0(P_{32}^p)J_0(Q_{32}^p), \tag{3b}$$

with

$$P_{3l}^\alpha=-2\frac{\mathbf{e}_\alpha\cdot(\mathbf{p}_{33}-\mathbf{p}_{ll})}{\mathbf{e}_\alpha\cdot\mathbf{p}_{3j}\omega_\alpha}\,\mathrm{Re}(\Omega_\alpha), \tag{4a}$$

$$Q_{3l}^\alpha=-2\frac{\mathbf{e}_\alpha\cdot(\mathbf{p}_{33}-\mathbf{p}_{ll})}{e_\alpha\cdot\mathbf{p}_{3j}\omega_\alpha}\,\mathrm{Im}(\Omega_\alpha), \tag{4b}$$

$(l=1,2;\ \alpha=p,j=1;\ \alpha=c,j=2)$. From the above expression, we expect that the PDM effect in the present problem takes a role if there is a nonzero difference between two diagonal dipole matrix elements $\mathbf{p}_{33}-\mathbf{p}_{jj}$. In addition, the amplitude and phase of the control field will both be important to the EIT property of the system because both $\rho_1$ and $\rho_2$ are dependent on $\mathrm{Re}(\Omega_c)$ and $\mathrm{Im}(\Omega_c)$.

The equation of motion of the density matrix reads

$$i\frac{\partial}{\partial t}\sigma_{11}-i\Gamma_{13}\sigma_{33}+\rho_1(\Omega_p^*\sigma_{31}-\Omega_p\sigma_{31}^*)=0, \tag{5a}$$

$$i\frac{\partial}{\partial t}\sigma_{22}-i\Gamma_{23}\sigma_{33}+\rho_2(\Omega_c^*\sigma_{32}-\Omega_c\sigma_{32}^*)=0, \tag{5b}$$

$$i\frac{\partial}{\partial t}\sigma_{33}+i\Gamma_3\sigma_{33}+\rho_1(\Omega_p\sigma_{31}^*-\Omega_p^*\sigma_{31})+\rho_2(\Omega_c\sigma_{32}^*-\Omega_c^*\sigma_{32})=0, \tag{5c}$$

$$\left(i\frac{\partial}{\partial t}+d_{21}\right)\sigma_{21}-\rho_1\Omega_p\sigma_{32}^*+\rho_2\Omega_c^*\sigma_{31}=0, \tag{5d}$$

$$\left(i\frac{\partial}{\partial t}+d_{31}\right)\sigma_{31}-\rho_1\Omega_p(\sigma_{33}-\sigma_{11})+\rho_2\Omega_c\sigma_{21}=0, \tag{5e}$$

$$\left(i\frac{\partial}{\partial t}+d_{32}\right)\sigma_{32}+\rho_1\Omega_p\sigma_{21}^*-\rho_2\Omega_c(\sigma_{33}-\sigma_{22})=0, \tag{5f}$$

with $\sigma_{jl}=A_jA_l^*$, $d_{21}=\Delta_2+i\gamma_{21}$, $d_{31}=\Delta_3+i\gamma_{31}$, and $d_{32}=(\Delta_3-\Delta_2)+i\gamma_{32}$. Here $\gamma_{jl}=(\Gamma_j+\Gamma_l)/2+\gamma_{jl}^{\rm col}$ $(j,l=1,2,3;j\neq l)$ and $\Gamma_j=\sum_{j<l}\Gamma_{jl}$, with $\Gamma_{jl}$ being the spontaneous emission decay rate from $|l\rangle$ to $|j\rangle$ and $\gamma_{jl}^{\rm col}$ being the dephasing rate reflecting the loss of phase coherence between $|j\rangle$ and $|l\rangle$ without changing of population.

The equation of motion for the probe field can be obtained by the Maxwell equation $\nabla^2\mathbf{E}-(1/c^2)\partial^2\mathbf{E}/\partial t^2=[1/(\varepsilon_0c^2)]\partial^2\mathbf{P}/\partial t^2$, with the polarization $\mathbf{P}$ given by

$$\mathbf{P}=N_m\left[\sum_{j=1}^{3}\mathbf{p}_{jj}\sigma_{jj}+\mathbf{p}_{13}\sigma_{31}e^{i\omega_p(z/c-t)}+\mathbf{p}_{23}\sigma_{32}e^{i\omega_c(z/c-t)}+\text{c.c.}\right]. \tag{6}$$

Under slowly varying envelope approximation, we obtain the equation of motion for $\Omega_p$:

$$i\left(\frac{\partial}{\partial z}+\frac{1}{c}\frac{\partial}{\partial t}\right)\Omega_p+\frac{\omega_p}{2c}\left(\frac{\partial^2}{\partial x^2}+\frac{\partial^2}{\partial y^2}\right)\Omega_p+\kappa_{13}\rho_1\sigma_{31}=0, \tag{7}$$

where $\kappa_{13}=N_m\omega_p|\mathbf{e}_p\cdot\mathbf{p}_{13}|^2/(2\varepsilon_0c\hbar)$.

We assume that the molecules are initially populated in the ground state $|1\rangle$. In the linear regime, the probe field is weak enough so that the ground state is not depleted during time evolution, i.e., $\sigma_{11}\approx1$ and $\sigma_{22}\approx\sigma_{33}\approx0$. In addition, we approximate that $J_0(P_{31}^p)\approx J_0(Q_{31}^p)\approx J_0(P_{32}^p)\approx J_0(Q_{32}^p)\approx1$. Third, for large beam radius the diffraction can be neglected. Taking into account the above approximations, Maxwell–Bloch (MB) equations (5) and (7) can be linearized. The solutions of $\sigma_{j1}$ $(j=2,3)$ and $\Omega_p$ are obtained as

$$\Omega_p=\int_{-\infty}^{\infty}d\omega F(\omega)e^{i[K(\omega)z-\omega t]}, \tag{8a}$$

$$\sigma_{j1}=\int_{-\infty}^{\infty}d\omega\frac{\alpha[(\omega+d_{21})\delta_{j3}-\beta\Omega_c^*\delta_{j2}]}{D(\omega)}F(\omega)e^{i[K(\omega)z-\omega t]} \tag{8b}$$

$(j=2,3)$, where $F(\omega)=(1/2\pi)\int_{-\infty}^{\infty}dt\Omega_p(0,t)e^{i\omega t}$ with $\Omega_p(0,t)$ being the probe field at the entrance of the medium, $D(\omega)=\beta^2|\Omega_c|^2-(\omega+d_{21})(\omega+d_{31})$, and

$$K(\omega)=\frac{\omega}{c}+\frac{\kappa_{13}\alpha^2(\omega+d_{21})}{D(\omega)} \tag{9}$$

is the linear dispersion relation of the system [36]. Factors $\alpha$ and $\beta$ are defined by

$$\alpha=J_0(P_{31}^c)J_0(Q_{31}^c), \tag{10a}$$

$$\beta=J_0(P_{32}^c)J_0(Q_{32}^c). \tag{10b}$$

We stress that this is because the occurrence of the factors $\alpha$ and $\beta$ make the EIT characters in the present system very different from those without PDMs, as shown below.

Shown in Fig. 2 is the linear dispersion relation $K(\omega)$ as a function of $\omega$ for $\Omega_c=1.0\times10^{12}$ s$^{-1}$. When plotting the figure, we have set $\Delta_2=\Delta_3=0$ for simplicity. The other system parameters used are based on HCN → HNC isomerization, which has often been used in theoretical studies of molecular dynamics [33]. In addition, the molecules are assumed to be prepared at very low temperature so that the inhomogeneous broadening of the molecular spectrum line due to the Doppler effect can be neglected. Specifically, we take $\gamma_{21}\approx1.0\times10^6$ s$^{-1}$, $\gamma_{31}\approx1.0\times10^{12}$ s$^{-1}$, $\kappa_{13}=1.0\times10^{12}$ cm$^{-1}$ s$^{-1}$, $\omega_p=1.943\times10^{15}$ s$^{-1}$, $\omega_c=9.92\times10^{14}$ s$^{-1}$, $\mathbf{p}_{11}=1.17\mathbf{p}_0$, $\mathbf{p}_{22}=-1.17\mathbf{p}_0$, $\mathbf{p}_{33}=1.18\mathbf{p}_0$, and $\mathbf{p}_{31}\approx\mathbf{p}_{32}=0.01\mathbf{p}_0$, with $|\mathbf{p}_0|=8.478\times10^{-28}$ C cm. These data will also be used in the following calculations.

From Fig. 2(a), we see that in the presence of the control field an EIT transparency window is opened. In addition, the dispersion property is also changed drastically in this EIT transparency window. In particular, the steep slope of Re($K$) results in a slow group velocity at the center frequency of the probe field. The large suppression of the absorption and reduction of the group velocity of the probe field are due to the quantum interference effect induced by the control field.

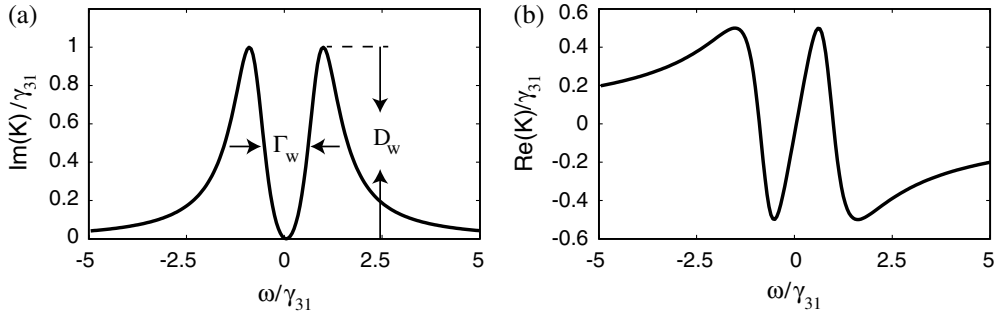


Fig. 2. Linear dispersion relation $K(\omega)$ as a function of $\omega$ for $\Omega_c=1.0\times10^{12}$ s$^{-1}$. (a) Imaginary part Im $K(\omega)$. (b) Real part Re $K(\omega)$. $\Gamma_W$ and $D_W$ are the width and depth of the EIT transparency window.

## 3. PHASE-DEPENDENT QUANTUM INTERFERENCE AND PHASE-CONTROLLED OPTICAL SWITCHING

The characters of the probe-field absorption spectrum can be described by two typical parameters. The first is the width of the EIT transparency window $\Gamma_w$, defined by the distance between two absorption peaks at half maxima [see Fig. 2(a)]. By the linear dispersion relation (9), one can obtain the expression of $\mathrm{Im}(K)$. Then it is easy to get

$$\Gamma_w = \sqrt{\gamma_{31}^2 + 4\beta^2|\Omega_c|^2} - \gamma_{31}. \tag{11}$$

The second is the depth of the EIT transparency window $D_w$, defined by the distance between the maximum of the absorption peak and the minimum of the EIT transparency window [see Fig. 2(a)]. We obtain

$$D_w = \frac{\kappa_{13}\alpha^2}{\gamma_{31}}. \tag{12}$$

Because both $\alpha$ and $\beta$ are functions of $\Omega_c$ through the zero-order Bessel function [see Eq. (10)], two pronounced characters of the EIT spectrum will appear: both $\Gamma_w$ and $D_w$ are oscillatory functions of the amplitude and the phase of the control field. To demonstrate this, we express $\Omega_c$ by its amplitude and phase, i.e., $\Omega_c = |\Omega_c|\exp(i\theta_c)$. Here $\theta_c$ is the phase difference between the phase of the control field passing through the atomic medium and its phase passing through the vacuum. Then, Eqs. (4a) and (4b) can be written as

$$P_{3j}^c = -2\frac{\mathbf{e}_c\cdot(\mathbf{p}_{33}-\mathbf{p}_{jj})}{\mathbf{e}_c\cdot\mathbf{p}_{32}\omega_c}|\Omega_c|\cos\theta_c, \tag{13a}$$

$$Q_{3j}^c = -2\frac{\mathbf{e}_c\cdot(\mathbf{p}_{33}-\mathbf{p}_{jj})}{e_c\cdot\mathbf{p}_{32}\omega_c}|\Omega_c|\sin\theta_c. \tag{13b}$$

We immediately obtain the following conclusions. First, $\alpha$ and $\beta$, and hence $\Gamma_w$ and $D_w$, are nonperiodically oscillatory functions of $|\Omega_c|$ if $\theta_c$ is fixed. Figures 3(a) and 3(b) show $\Gamma_w$ and $D_w/\gamma_{31}$ as functions of $|\Omega_c|/\gamma_{31}$ for $\theta_c = 0$, respectively. One sees that $\Gamma_W$ ($D_W$) varies periodically with $|\Omega_c|$ and its amplitude increases (decreases) as $|\Omega_c|$ grows. Such character has been indicated implicitly in Ref. [34]. Second, $\alpha$ and $\beta$, and hence $\Gamma_w$ and $D_w$, are periodically oscillatory functions of $\theta_c$ if $|\Omega_c|$ is fixed. Shown in Figs. 3(c) and 3(d) are $\Gamma_w/\gamma_{31}$ and $D_w$ as functions of $\theta_c$ for $|\Omega_c|/\gamma_{31} = 5.05$ and $1.19\times10^3$, respectively.

The above EIT characters inherent in the system are very different from those without PDMs, where both $\Gamma_w$ and $D_w$ do not depend on $\theta_c$. This means that a *phase-dependent quantum interference effect* can occur in the molecular system with PDMs.

In most operation conditions, $K(\omega)$ can be Taylor expanded around the center frequency $\omega_p$ of the probe field, that is, $\omega = 0$ [36]. We thus have $K(\omega) = K_0 + K_1\omega + \frac{1}{2}K_2\omega^2 + \cdots$, where $K_j = [\partial^j K(\omega)/\partial\omega^j]|_{\omega=0}$ ($j = 0, 1, 2, \ldots$). These dispersion coefficients can be obtained analytically by using Eq. (9). Here, $K_0 = \mathrm{Re}(K_0) + i\,\mathrm{Im}(K_0)$ gives the phase shift $\mathrm{Re}(K_0)$ per unit length and absorption coefficient $2\,\mathrm{Im}(K_0)$ of the probe-field intensity, $V_g = 1/\mathrm{Re}(K_1)$ determines the group velocity, and $K_2$ describes the group-velocity dispersion (i.e., the pulse spreading and attenuation). For the probe pulse with a Gaussian input form, i.e., $\Omega_p(0,t) = \Omega_p(0,0)\exp(-t^2/\tau_0^2)$, we have the solution

$$\Omega_p(z,t) = \frac{\Omega_p(0,0)}{\sqrt{c_1(z)-ic_2(z)}}\exp\left[iK_0z - \frac{(K_1z-t)^2}{[c_1(z)-ic_2(z)]\tau_0^2}\right], \tag{14}$$

by keeping terms up to $\omega^2$ in the Taylor expansion, where $c_1(z) = 1 + 2z\,\mathrm{Im}(K_2)/\tau_0^2$ and $c_2(z) = 2z\,\mathrm{Re}(K_2)/\tau_0^2$. It is clear that for the probe pulse with a long pulse length $\tau_0$, $c_1(z) \approx 1$

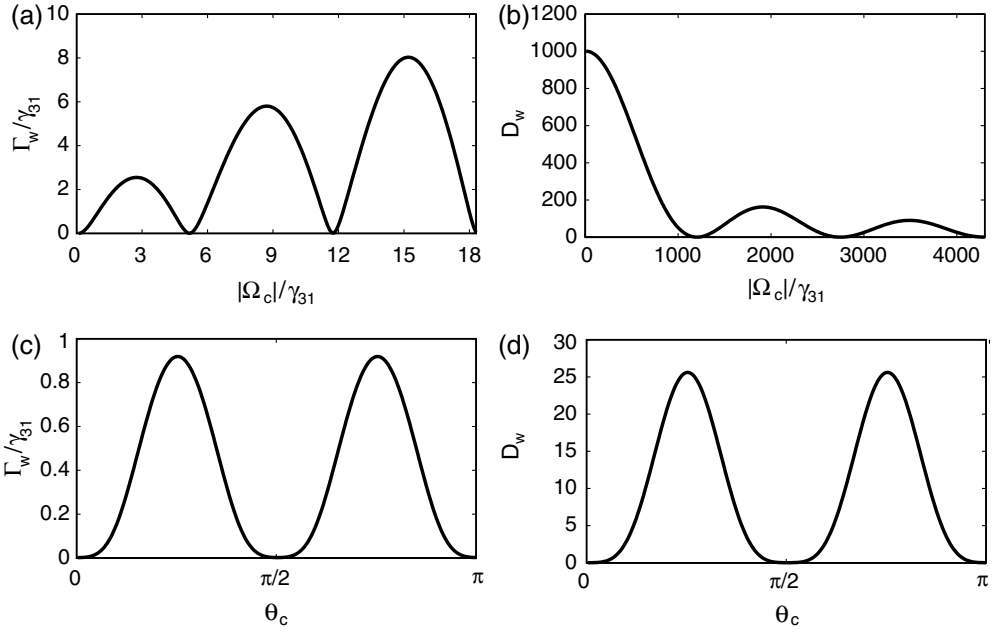


Fig. 3. (a) $\Gamma_w/\gamma_{31}$ as a function of $|\Omega_c|/\gamma_{31}$ for $\theta_c = 0$. (b) $D_w$ as a function of $|\Omega_c|/\gamma_{31}$ for $\theta_c = 0$. (c) $\Gamma_w/\gamma_{31}$ as a function of $\theta_c$ for $|\Omega_c|/\gamma_{31} = 5.05$. (d) $D_w$ as a function of $\theta_c$ for $|\Omega_c|/\gamma_{31} = 1.19\times10^3$.

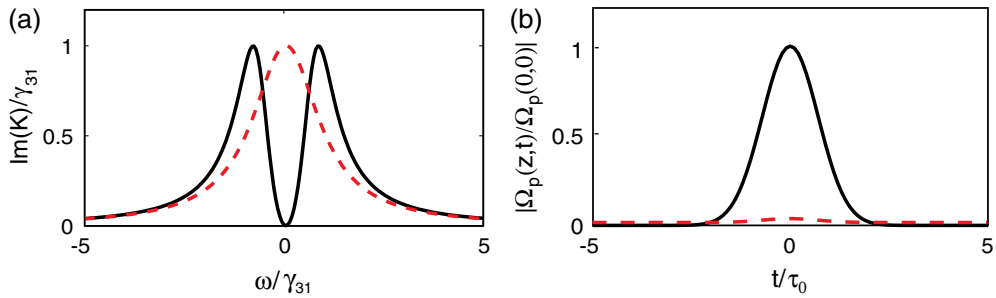


Fig. 4. (a) $\mathrm{Im}K(\omega)$ as a function of $\omega/\gamma_{31}$ for $\Omega_c/\gamma_{31}=5.05e^{i\pi/4}$ (solid line) and $\Omega_c/\gamma_{31}=5.05$ (dashed line). (b) Output of probe pulse with $\tau_0=1.0\times10^{-8}$ s after passing through the molecular medium of length 4 cm. The solid line (corresponding to switching on) and dashed line (corresponding to switching off) are the output wave shapes of $|\Omega_p(z,t)/\Omega_p(0,0)|$ for $\theta_c=\pi/4$ and $\theta_c=0$, respectively.

and $c_2(z)\approx0$, and hence a shape-preserving propagation can be realized.

An optical switch is a device by which a pulse of light at one frequency will cause the absorption of light at another frequency [37]. In recent years, the optical switch at low light level based on the quantum interference effect has been of great interest due to its important applications in optical and quantum information science [37–43]. However, in most studies up to date switching of one laser field is realized by changing the amplitude of another laser field.

Here, we suggest to design a new type of optical switch for the probe field caused by the phase change of the control field by using the phase-controlled quantum interference character of the present molecular system with PDMs. Shown in Fig. 4(a) is the probe is the probe absorption spectrum $\mathrm{Im}K(\omega)$ as a function of $\omega/\gamma_{31}$ for $\Omega_c/\gamma_{31}=5.05e^{i\pi/4}$ (solid line) and $\Omega_c/\gamma_{31}=5.05$ (dashed line). We see that the EIT transparency window closes completely when the phase of the control field $\theta_c$ decreases from $\pi/4$ to 0. Shown in Fig. 4(b) is the output of the probe pulse with $\tau_0=1.0\times10^{-8}$ s after passing through the molecular medium of length 4 cm. The solid line (corresponding to switching on) and dashed line (corresponding to switching off) in the figure are the output wave shapes of $|\Omega_p(z,t)/\Omega_p(0,0)|$ for $\theta_c=\pi/4$ and $\theta_c=0$, respectively. One sees that a phase-controlled optical switch is indeed easily realized in our system.

The efficiency of the optical switch can be defined as $\eta=(I_{\mathrm{close}}-I_{\mathrm{open}})/I_{\mathrm{in}}$. Here $I_{\mathrm{in}}$ is the incident light intensity, $I_{\mathrm{close}}$ is the transmitted intensity when the switch is closed, and $I_{\mathrm{open}}$ is the transmitted intensity when the switch is open. In the present system, $\eta$ can reach nearly to 100% for the medium length around 4 cm. In comparison with the phase-controlled optical switch realized in an atomic system proposed in Ref. [44], where a four-level atomic gas and four laser fields are required, the optical switch suggested in the present scheme is much simpler because fewer resources are needed.

## 4. ENHANCED KERR NONLINEARITY AND SOLITONS

### A. Enhanced Kerr Nonlinearity

From the solution (14), it is easy to see that large group-velocity dispersion will contribute to both spreading and attenuation of the probe pulse if the pulse length $\tau_0$ is short, which is undesirable in practical applications. In the following, we show that it is possible to realize a shape-conserved propagation of the probe field in the molecular system by using the nonlinear effect to balance the group-velocity dispersion.

We first calculate the susceptibility of the probe field, which is defined as

$$\chi_p=\frac{N_m\rho_1|\mathbf{p}_{31}\cdot\mathbf{e}_p|^2}{\varepsilon_0\hbar}\frac{\sigma_{31}}{\Omega_p}=\chi_p^{(1)}+\chi_p^{(3)}|E_p|^2, \tag{15}$$

where $\chi_p^{(1)}$ is the first-order susceptibility describing the linear property and $\chi_p^{(3)}$ is the third-order one characterizing the Kerr nonlinearity of the system.

By solving Eqs. (5) under steady-state approximation, we obtain

$$\chi_p^{(1)}=\frac{N_m|\mathbf{e}_p\cdot\mathbf{p}_{13}|^2}{\varepsilon_0\hbar}T_1, \tag{16a}$$

$$\chi_p^{(3)}=\frac{N_m|\mathbf{e}_p\cdot\mathbf{p}_{13}|^4}{\varepsilon_0\hbar^3}\frac{iJ_1(T_1-\mathrm{c.c.})+iJ_2(d_{32}T_2-\mathrm{c.c.})+\alpha^2T_2}{d_{32}^*(\beta^2|\Omega_c|^2-d_{21}d_{31})}, \tag{16b}$$

with

$$\begin{aligned}
T_1&=\alpha\frac{\Delta_2}{\beta^2|\Omega_c|^2-d_{21}d_{31}},\\
T_2&=\alpha\frac{\beta^2|\Omega_c|^2-id_{31}\gamma_{21}}{\beta^2|\Omega_c|^2-d_{21}d_{31}},\\
J_1&=\alpha^2\left[(\beta^2|\Omega_c|^2+d_{21}d_{32}^*)\frac{4\beta^2|\Omega_c|^2+\gamma_{31}^2}{2\gamma_{31}\beta^2|\Omega_c|^2}-\frac{2\beta^2|\Omega_c|^2-d_{21}d_{32}^*}{\gamma_{31}}\right],\\
J_2&=\alpha^2\frac{\beta^2|\Omega_c|^2+d_{21}d_{32}^*}{2\gamma_{31}\beta^2|\Omega_c|^2}.
\end{aligned} \tag{17}$$

We note that the third-order susceptibility $\chi_p^{(3)}$ can be greatly enhanced by selecting suitable system parameters (making $\beta^2|\Omega_c|^2-d_{21}d_{31}$ small). Shown in Figs. 5(a) and 5(b) are the real and imaginary parts of the third-order susceptibility, i.e., $\mathrm{Re}[\chi_p^{(3)}]$ and $\mathrm{Im}[\chi_p^{(3)}]$, as functions of the two-photon detuning $\Delta_2/\gamma_{31}$. The system parameters are taken as $\kappa_{13}=10^{14}\ \mathrm{cm^{-1}\,s^{-1}}$, $\Omega_c/\gamma_{31}=0.1$, and $\Delta_3/\gamma_{31}=1.0$ with the other parameters being the same as those used in Fig. 2. We note that at $\Delta_2=0$, where the system is under an exact EIT, no nonlinearity exists. Therefore, to have a nonzero nonlinear effect a deviation from the exact EIT is necessary. We also note that in the figure the real part of $\chi_p^{(3)}$ is smaller than the corresponding imaginary part in a large domain; however, the real part of $\chi_p^{(3)}$ can be much larger than the corresponding imaginary part when $\Delta_2/\gamma_{31}$ is very close to zero, i.e., the

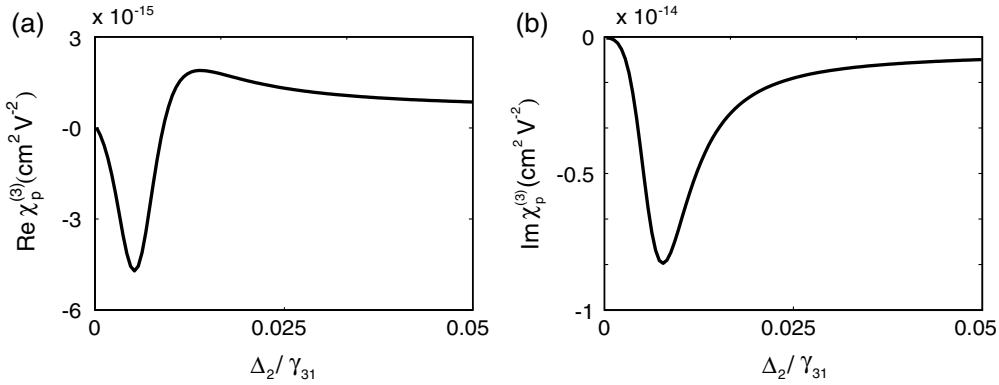


Fig. 5. (a) $\mathrm{Re}[\chi_p^{(3)}]$ as a function of $\Delta_2/\gamma_{31}$. (b) $\mathrm{Im}[\chi_p^{(3)}]$ as a function of $\Delta_2/\gamma_{31}$. The system parameters are given in the text. The condition that $\mathrm{Re}[\chi_p^{(3)}] \gg \mathrm{Im}[\chi_p^{(3)}]$ can be satisfied when $\Delta_2/\gamma_{31} \ll 1$.

condition that $\mathrm{Re}[\chi_p^{(3)}] \gg \mathrm{Im}[\chi_p^{(3)}]$ can be satisfied when $\Delta_2/\gamma_{31} \ll 1$. For example, when taking $\Delta_2/\gamma_{31} = 0.002$, we obtain $\chi_p^{(3)} = -(0.15 + i0.04) \times 10^{-14}$ cm$^2$ V$^{-2}$. The physical reason for the enhanced Kerr nonlinearity comes from the fact that the system is highly resonant and works nearly under the EIT condition. The enhanced Kerr effect is useful to form optical solitons, as shown below.

### B. Nonlinear Envelope Equation

To study the nonlinear evolution of the probe pulse, we apply the method of multiple scales to solve the MB Eqs. (5) and (7). We take the following asymptotic expansions $\sigma_{jk} = \delta_{j1}\delta_{k1} + \sum_{l=1}^{\infty} \epsilon^l \sigma_{jk}^{(l)}$ $(j,k = 1,2,3;$ both $\delta_{j1}$ and $\delta_{k1}$ are Kronecker delta symbols) and $\Omega_p = \sum_{l=1}^{\infty} \epsilon^l \Omega_p^{(l)}$, where $\epsilon$ is a dimensionless small parameter characterizing the amplitude of the probe field. All quantities on the right-hand side of the expansions are considered as functions of the multiscale variables $z_l = \epsilon^l z$ $(l = 0,1,2)$, $t_1 = \epsilon t$, $x_1 = \epsilon x$, and $y_1 = \epsilon y$.

Substituting the expansions into Eqs. (5) and (7), and comparing the coefficients of $\epsilon^l$ $(l = 1,2,3\ldots)$, we obtain a set of linear but inhomogeneous equations that can be solved order by order. At leading order $(l = 1)$, we have the solution in the linear regime, which is the same as that given in Eq. (8), but now $F$ is taken to be a function of the slow variables $t_2, x_1, y_1, z_1$, and $z_2$.

At the next order $(l = 2)$, a divergence-free condition requires $\partial F/\partial z_1 + (1/V_g)(\partial F/\partial t_1) = 0$. The second-order solution reads $\sigma_{31}^{(2)} = \sigma_{21}^{(2)} = 0$, $\sigma_{jj}^{(2)} = a_{jj}^{(2)}|F|^2 e^{-\tilde{\alpha} z_2}$ $(j = 1,2)$, and $\sigma_{32}^{(2)} = a_{32}^{(2)}|F|^2 e^{-\tilde{\alpha} z_2}$, where

$$a_{11}^{(2)} = \alpha^2 \frac{[i\Gamma_{23} - 2\beta^2|\Omega_c|^2(1/d_{32} - 1/d_{32}^*)]X - i\Gamma_{13}\beta^2|\Omega_c|^2[1/(Dd_{32}^*) - 1/(D^* d_{32})]}{i\Gamma_{13}\beta^2|\Omega_c|^2(1/d_{32} - 1/d_{32}^*)},$$

$$a_{22}^{(2)} = \frac{\alpha^2 X - i\Gamma_{13} a_{11}^{(2)}}{i\Gamma_{13}}, \quad a_{32}^{(2)} = \frac{\beta\Omega_c}{d_{32}}\left[\frac{\alpha^2}{D^*} - (a_{11}^{(2)} + 2a_{22}^{(2)})\right], \tag{18}$$

and $\tilde{\alpha} = \epsilon^{-2}\alpha = \epsilon^{-2}\,\mathrm{Im}[K(\omega)]$, with $X = (\omega + d_{21}^*)/D^* - (\omega + d_{21})/D$.

With the above results we proceed to the third order $(l = 3)$. The divergence-free condition in this order yields the nonlinear equation for the envelope function $F$:

$$i\frac{\partial F}{\partial z_2} - \frac{K_2}{2}\frac{\partial^2 F}{\partial t_1^2} + \frac{c}{2\omega_p}\left(\frac{\partial^2}{\partial x_1^2} + \frac{\partial^2}{\partial y_1^2}\right)F - W|F|^2 F e^{-2\tilde{\alpha} z_2} = 0, \tag{19}$$

where

$$W = -\kappa_{13}\alpha \frac{\beta\Omega_c a_{32}^{(2)*} + (\omega + d_{21})(2a_{11}^{(2)} + a_{22}^{(2)})}{D(\omega)},$$

characterizes the self-phase modulation (SPM) effect of the system. For obtaining a nonzero real part of $W$ around $\omega = 0$, it is necessary to require that $\Delta_2 \neq 0$, which is also required for a nonzero real part of $\chi_p^{(3)}$.

Combining equations in all orders and taking $\tau = t - z/V_g$, $\Omega_p \approx \varepsilon F e^{iK_0 z} = U e^{iK_0 z}$, we arrive at the equation

$$i\left(\frac{\partial}{\partial z} + \frac{\alpha}{2}\right)U - \frac{K_2}{2}\frac{\partial^2 U}{\partial \tau^2} + \frac{c}{2\omega_p}\left(\frac{\partial^2}{\partial x^2} + \frac{\partial^2}{\partial y^2}\right)U - W|U|^2 U = 0. \tag{20}$$

### C. Slow-Light Solitons

The formation and propagation of an optical soliton in the system requires the following conditions: (i) there is a balance between the dispersion and nonlinearity, and (ii) the absorption of the probe field is negligibly small. In general, coefficients of the envelope Eq. (20) are complex, which means that a soliton solution, even if it exists and is produced, may be highly unstable during propagation. However, if a realistic set of system parameters under some condition can be found so that the imaginary part of these coefficients can be much smaller than their corresponding real part, it is possible to get a shape-preserving, localized solution that

can propagate a rather long distance without a significant distortion. In the present system, the condition of relatively small imaginary parts of the coefficients can be achieved by the EIT condition.

Under this condition, Eq. (20) with neglect of the small imaginary part of the coefficients can be written in the dimensionless form

$$i\frac{\partial u}{\partial \zeta}+s_1\frac{\partial^2 u}{\partial \sigma^2}+2s_2|u|^2u=-id_0u-d_1\left(\frac{\partial^2}{\partial \xi^2}+\frac{\partial^2}{\partial \eta^2}\right)u, \quad (21)$$

where $U=U_0u$, $z=-2L_D\zeta$, $\tau=\tau_0\sigma$, $(x,y)=R_\perp(\xi,\eta)$, $s_1=\mathrm{sign}(K_{2r})$ (here and in the following the subscript "$r$" means real part), $s_2=\mathrm{sign}(W_r)$, $d_0=L_D/L_0$, and $d_1=L_D/L_1$. Here $L_0=2/\alpha$ is the characteristic absorption length, $L_D=\tau_0^2/|K_{2r}|$ is the characteristic dispersion length, $L_1=\omega_pR_\perp^2/c$ is the characteristic diffraction length, and $L_{NL}=1/(|W_r|U_0^2)$ is the characteristic nonlinearity length with $U_0$ being the typical Rabi frequency of the probe field. In order to obtain Eq. (21), we have imposed the condition $L_D=L_{NL}$; i.e., a balance between the dispersion and nonlinearity is achieved.

If $d_0\ll 1$ ($L_D\ll L_0$) and $d_1\ll 1$ ($L_D\ll L_1$), the terms on the right-hand side of Eq. (21) can be regarded as small perturbations and can be neglected in the first order. Thus, Eq. (21) reduces to the standard NLS equation reading $i\partial u/\partial\zeta+s_1\partial^2u/\partial\sigma^2+2s_2\varsigma|u|^2u=0$, which permits the bright soliton solution $u=\mathrm{sech}\,\sigma e^{i\zeta}$ for $s_1s_2=1$ and the dark soliton solution $u=\tanh\sigma e^{i\zeta}$ for $s_1s_2=-1$. Returning to the original variables, the bright and dark soliton solutions have the form

$$\Omega_p^{\mathrm{bright}}=\frac{1}{\tau_0}\sqrt{\frac{K_{2r}}{W_r}}\,\mathrm{sech}\left[\frac{1}{\tau_0}\left(t-\frac{z}{V_g}\right)\right]\exp\left(iK_0z-i\frac{z}{2L_D}\right), \quad (22a)$$

$$\Omega_p^{\mathrm{dark}}=\frac{1}{\tau_0}\sqrt{\frac{K_{2r}}{W_r}}\tanh\left[\frac{1}{\tau_0}\left(t-\frac{z}{V_g}\right)\right]\exp\left(iK_0z-i\frac{z}{2L_D}\right), \quad (22b)$$

respectively.

Now we present a numerical example for the solitons given above. We take $\kappa_{13}=10^{14}\ \mathrm{cm^{-1}\,s^{-1}}$, $\Delta_2/\gamma_{31}=0.1$, $\Delta_3/\gamma_{31}=6.0$, $\Omega_c/\gamma_{31}=2.0$, $\tau_0=2.24\times10^{-9}$ s, $U_0=5.26\times10^8\ \mathrm{s^{-1}}$, and $R_\perp=1.2\times10^{-2}$ cm; the other parameters are the same as those used in Fig. 2. With the above parameters, we obtain that $K_0\approx1.10+i0.19\ \mathrm{cm^{-1}}$, $K_1\approx(1.19+i0.27)\times10^{-8}\,\mathrm{cm^{-1}s}$, $K_2\approx(1.67+i0.34)\times10^{-18}\ \mathrm{cm^{-1}\,s^2}$, and $W\approx-(1.20+i0.15)\times10^{-18}\ \mathrm{cm^{-1}\,s^2}$. The characteristic lengths are $L_0\approx10.8$ cm, $L_D=L_{NL}\approx3.0$ cm, and $L_{Diff}\approx12.9$ cm, and hence $d_0\approx0.28$ and $d_1\approx0.32$. Using these parameters, we obtain the group velocity of the probe-field envelope

$$V_g\approx2.8\times10^{-3}\ c, \quad (23)$$

which is much smaller than the light speed in the vacuum (i.e., $c$). Because $s_1s_2=-1$, the soliton obtained under the above parameters is an ultraslow dark soliton.

In Figs. 6(a) and 6(b) we show the evolution of the probe intensity $|\Omega_p/U_0|^2$ by directly integrating Eq. (21). The initial condition is given by the slow-light dark soliton solution (22b) embedded in a wide Gaussian background. The stability of the soliton is checked by adding a small random noise (5%) to the initial condition and evolving them. We see that the slow-light dark soliton is rather robust during propagation to $z=2L_D\approx6$ cm. A slight deformation of the slow-light soliton due to the absorption and diffraction can also be observed when $z>L_D$.

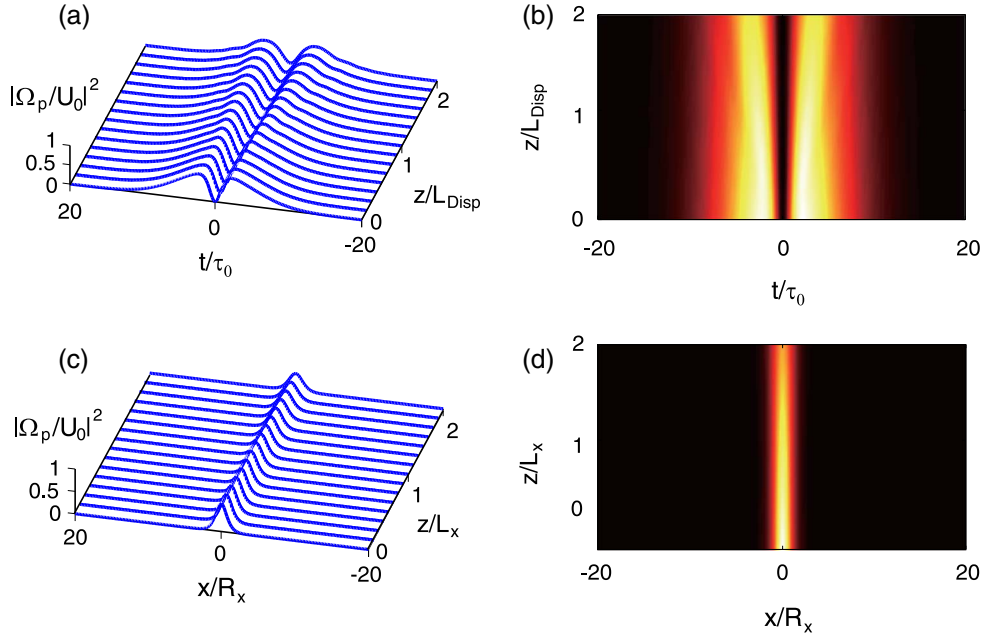


Fig. 6. Evolution of the intensity $|\Omega_p/U_0|^2$ by directly integrating Eq. (21). (a), (b) (intensity pattern in $t$–$z$ plane) Evolution of the slow-light dark soliton. The initial condition is given by the solution (22b) embedded in a wide Gaussian background. (c), (d) (intensity pattern in $x$–$z$ plane) Evolution of the weak-light bright soliton. The initial condition is given by the solution (25a). In all panels, the stability of solitons is checked by adding a small random noise to the initial condition and evolving them. The system parameters are given in the text.

### D. Weak-Light Spatial Solitons

If the probe pulse duration $\tau_0$ is much longer than $2.24\times10^{-9}$ s, the dispersion of the system will not be able to balance the nonlinearity, and hence we cannot find stable ultraslow optical solitons. In this regime, however, we can consider the possibility of the formation of spatial optical solitons in the system. The physical mechanism of realizing spatial solitons is the interplay and balance between diffraction and nonlinearity.

For a weak probe field with transverse radii $R_x \ll R_y$ ($R_x$ and $R_y$ are, respectively, the probe beam radii in the $x$ and $y$ directions), only the diffraction in the $x$ direction is significant. In this case Eq. (20) can be reduced to the form

$$i\frac{\partial u}{\partial \zeta}+\frac{\partial^2 u}{\partial \xi^2}+2s_2|u|^2u=id_0u+\left(d_1\frac{\partial^2}{\partial \eta^2}+d_2\frac{\partial^2}{\partial o^2}\right)u, \quad (24)$$

where $z=2L_x\zeta$, $(x,y)=(R_x\xi,R_y\eta)$, $d_0=L_x/L_0$, $d_1=L_x/L_y$, and $d_2=L_x/L_{\mathrm{D}}$. Here $L_x=\omega_pR_x^2/c$ is the characteristic diffraction length in the $x$ direction and $L_y=\omega_pR_y^2/c$ is the characteristic diffraction length in the $y$ direction. When obtaining Eq. (24), we have imposed the condition $L_x=L_{\mathrm{NL}}$; i.e., a balance between the diffraction in the $x$ direction and nonlinearity is achieved.

If $d_0\ll1$ ($L_x\ll L_0$), $d_1\ll1$ ($L_x\ll L_y$), and $d_2\ll1$ ($L_x\ll L_{\mathrm{D}}$), the terms on the right-hand side of Eq. (24) can be regarded as small perturbations and can be neglected in the first order. Thus, Eq. (24) reduces to the standard NLS equation reading $i\partial u/\partial\zeta+\partial^2u/\partial\xi^2+2s_2|u|^2u=0$, which permits the bright soliton solution $u=\operatorname{sech}\xi e^{i\zeta}$ for $s_2=1$ and the dark soliton solution $u=\tanh\xi e^{i\zeta}$ for $s_2=-1$. Returning to the original variables, the single bright and dark soliton solutions read

$$\Omega_p^{\mathrm{bright}}=\frac{1}{R_x}\sqrt{\frac{c}{\omega_pW_r}}\operatorname{sech}\left(\frac{x}{R_x}\right)\exp\left(iK_0z-i\frac{z}{2L_x}\right), \quad (25a)$$

$$\Omega_p^{\mathrm{dark}}=\frac{1}{R_x}\sqrt{\frac{c}{\omega_pW_r}}\tanh\left(\frac{x}{R_x}\right)\exp\left(iK_0z-i\frac{z}{2L_x}\right), \quad (25b)$$

respectively.

For a practical example, we take $\tau_0=4.48\times10^{-9}$ s, $R_x=6.8\times10^{-3}$ cm, and $R_y=R_\perp=1.2\times10^{-2}$ cm; the other parameters are the same as those used in Figs. 6(a) and 6(b). With the above parameters, we obtain that $L_{\mathrm{D}}\approx12.0$ cm, $L_x\approx3.0$ cm, and $L_y\approx9.3$ cm, which leads to $d_0\approx0.28$, $d_1\approx0.32$, and $d_2\approx0.25$. Because in this situation $s_2=1$, the soliton obtained is a bright one [i.e., Eq. (25a)].

In Figs. 6(c) and 6(d) we show the evolution of the probe intensity $|\Omega_p/U_0|^2$ by directly integrating Eq. (24). The initial condition is provided by the bright soliton solution (25a). The stability of the soliton is checked by adding a small random noise to the initial condition and evolving them. We see that the bright soliton is rather robust during the propagation distance of $z=2L_{\mathrm{D}}\approx6$ cm.

Using Poynting's vector, it is easy to estimate the peak power for generating the optical soliton described above, which reads

$$P_{\max}\approx18.53\ \mathrm{W}, \quad (26)$$

with the cross-sectional area of the probe beam being taken as $S_0\approx R_xR_y$. We note that the peak power for generating the soliton in the present molecular system is higher than that in the atomic systems [16–18,45]. This is because the electric-dipole matrix element $\mathbf{p}_{31}$ of the present molecular system is about three orders smaller than that of the atomic systems. However, this is still a drastic contrast to conventional media such as glass-based optical fibers, where picosecond or femtosecond laser pulses are usually needed to reach a very high peak power from kilowatts to megawatts to bring out the enough nonlinear effect required for the formation of spatial optical solitons [46,47].

## 5. SUMMARY

In conclusion, we have investigated the linear and nonlinear light pulse propagations in a three-level Λ-type molecular system with PDMs via EIT. We have found that the EIT characters in such a system depend strongly on the phase of control field, based on which a phase-controlled optical switching can be designed. We have shown that the Kerr nonlinearity of the system can be largely enhanced due to the control-field-induced quantum interference effect. We have derived the NLS equation for the evolution of the probe-field envelope and demonstrated that it is possible to realize stable slow- and weak-light solitons in the system. The results obtained in this work may guide a relevant experiment and have potential applications in the field of optical information communication and processing.

## ACKNOWLEDGMENTS

This work was supported by NSF-China under grant nos. 1174080 and 11105052, and by the Open Fund from the State Key Laboratory of Precision Spectroscopy, ECNU.

## REFERENCES AND NOTE

1. M. Fleischhauer, A. Imamoğlu, and J. P. Marangos, "Electromagnetically induced transparency: optics in coherent media," Rev. Mod. Phys. **77**, 633–673 (2005), and references therein.
2. L. V. Hau, S. E. Harris, Z. Dutton, and C. H. Behrrozi, "Light speed reduction to 17 meters per second in an ultracold atomic gas," Nature **397**, 594–598 (1999).
3. M. M. Kash, V. A. Sautenkov, A. S. Zibrov, L. Hollberg, G. R. Welch, M. D. Lukin, Y. Rostovtsev, E. S. Fry, and M. O. Scully, "Ultra-slow light and enhanced nonlinear optical effects in a coherently driven hot atomic gas," Phys. Rev. Lett. **82**, 5229–5232 (1999).
4. H. Schmidt and A. Imamoğlu, "Giant Kerr nonlinearities obtained by electromagnetically induced transparency," Opt. Lett. **21**, 1936–1938 (1996).
5. H. Kang and Y. Zhu, "Observation of large Kerr nonlinearity at low light intensities," Phys. Rev. Lett. **91**, 093601 (2003).
6. C. Liu, Z. Dutton, C. H. Behroozi, and L. V. Hau, "Observation of coherent optical information storage in an atomic medium using halted light pulses," Nature **409**, 490–493 (2001).
7. A. I. Lvovsky, B. C. Sanders, and W. Tittel, "Optical quantum memory," Nat. Photonics **3**, 706–714 (2009).
8. M. D. Lukin, P. R. Hemmer, M. Löffler, and M. O. Scully, "Resonant enhancement of parametric processes via radiative interference and induced coherence," Phys. Rev. Lett. **81**, 2675–2678 (1998).
9. R. Santra, E. Arimondo, T. Ido, C. H. Greene, and J. Ye, "High-accuracy optical clock via three-level coherence in neutral bosonic $^{88}$Sr," Phys. Rev. Lett. **94**, 173002 (2005).
10. C. Ottaviani, D. Vitali, M. Artoni, F. Cataliotti, and P. Tombesi, "Polarization qubit phase gate in driven atomic media," Phys. Rev. Lett. **90**, 197902 (2003).

11. C. Hang, Y. Li, L. Ma, and G. Huang, "Three-way entanglement and three-qubit phase gate based on a coherent six-level atomic system," Phys. Rev. A **74**, 012319 (2006).
12. Y. Wu and L. Deng, "Ultraslow optical solitons in a cold four-state medium," Phys. Rev. Lett. **93**, 143904 (2004).
13. G. Huang, L. Deng, and M. G. Payne, "Dynamics of ultraslow optical solitons in a cold three-state atomic system," Phys. Rev. E **72**, 016617 (2005).
14. C. Hang, G. Huang, and L. Deng, "Generalized nonlinear Schrodinger equation and ultra slow optical solitons in a cold four-state atomic system," Phys. Rev. E **73**, 036607 (2006).
15. C. Hang and G. Huang, "Weak-light ultraslow vector solitons via electromagnetically induced transparency," Phys. Rev. A **77**, 033830 (2008).
16. H. Michinel, M. J. Paz-Alonso, and V. M. Pérez-García, "Turning light into a liquid via atomic coherence," Phys. Rev. Lett. **96**, 023903 (2006).
17. C. Hang, G. Huang, and L. Deng, "Stable high-dimensional spatial weak-light solitons in a resonant three-state atomic system," Phys. Rev. E **74**, 046601 (2006).
18. C. Hang, V. V. Konotop, and G. Huang, "Spatial solitons and instabilities of light beams in a three-level atomic medium with a standing-wave control field," Phys. Rev. A **79**, 033826 (2009).
19. Y. Zhang, Z. Wang, H. Zheng, C. Yuan, C. Li, K. Lu, and M. Xiao, "Four-wave-mixing gap solitons," Phys. Rev. A **82**, 053837 (2010).
20. Y. Zhang, Z. Wang, Z. Nie, C. Li, H. Chen, K. Lu, and M. Xiao, "Four-wave mixing dipole soliton in laser-induced atomic gratings," Phys. Rev. Lett. **106**, 093904 (2011).
21. J. Qi, F. C. Spano, T. Kirova, A. Lazoudis, J. Magnes, L. Li, L. M. Narducci, R. W. Field, and A. M. Lyyra, "Measurement of transition dipole moments in lithium dimers using electromagnetically induced transparency," Phys. Rev. Lett. **88**, 173003 (2002).
22. J. Qi and A. M. Lyyra, "Electromagnetically induced transparency and dark fluorescence in a cascade three-level diatomic lithium system," Phys. Rev. A **73**, 043810 (2006).
23. A. Lazoudis, T. Kirova, E. H. Ahmed, L. Li, J. Qi, and A. M. Lyyra, "Electromagnetically induced transparency in an open Λ-type molecular lithium system," Phys. Rev. A. **82**, 023812 (2010).
24. L. Li, P. Qi, A. Lazoudis, E. Ahmed, and A. M. Lyyra, "Observation of electromagnetically induced transparency in two-photon transitions of K239," Chem. Phys. Lett. **403**, 262–267 (2005).
25. A. Lazoudis, E. H. Ahmed, L. Li, T. Kirova, P. Qi, A. Hansson, J. Magnes, and A. M. Lyyra, "Experimental observation of the dependence of Autler–Townes splitting on the probe and coupling laser wave-number ratio in Doppler-broadened open molecular cascade systems," Phys. Rev. A **78**, 043405 (2008).
26. A. Lazoudis, T. Kirova, E. H. Ahmed, P. Qi, J. Huennekens, and A. M. Lyyra, "Electromagnetically induced transparency in an open V-type molecular system," Phys. Rev. A **83**, 063419 (2011).
27. S. Ghosh, J. E. Sharping, D. G. Ouzounov, and A. L. Gaeta, "Resonant optical interactions with molecules confined in photonic band-gap fibers," Phys. Rev. Lett. **94**, 093902 (2005).
28. F. Benabid and P. J. Roberts, "Linear and nonlinear optical properties of hollow core photonic crystal fiber," J. Mod. Opt. **58**, 87–124 (2011).
29. P. S. Light, F. Benabid, G. J. Pearce, F. Couny, and D. M. Bird, "Electromagnetically induced transparency in acetylene molecules with counter propagating beams in V and Λ schemes," Appl. Phys. Lett. **94**, 141103 (2009).
30. C. Tan, C. Zhu, and G. Huang, "Analytical approach on linear and nonlinear pulse propagations in an open Λ-type molecular system with Doppler broadening," J. Phys. B **46**, 025103 (2013).
31. C. Zhu, C. Tan, and G. Huang, "Crossover from electromagnetically induced transparency to Autler–Townes splitting in open V-type molecular systems," Phys. Rev. A **87**, 043813 (2013).
32. C. A. Marx and W. Jakubetz, "Phase-sensitive stimulated Raman adiabatic passage in dipolar extended lambda systems," J. Chem. Phys. **125**, 234103 (2006).
33. A. Brown, "Effect of permanent dipole moments on stimulated Raman adiabatic passage," Chem. Phys. **342**, 16–24 (2007), and references therein.
34. F. Zhou, Y. Niu, and S. Gong, "Electromagnetically induced transparency in a three-level lambda system with permanent dipole moments," J. Chem. Phys. **131**, 034105 (2009).
35. G. Ma, B. Shi, Y. Yao, H. Guo, and W. Liu, "Permanent dipole moments induced new coherent effects in absorption and dispersion of a three-level molecule," J. Mod. Opt. **57**, 390–394 (2010).
36. The frequency and wave number of the probe field in the molecular medium are given by $\omega_p + \omega$ and $k_p + K(\omega)$, respectively. Thus $\omega = 0$ corresponds to the center frequency of the probe field.
37. S. E. Harris and Y. Yamamoto, "Photon switching by quantum interference," Phys. Rev. Lett. **81**, 3611–3614 (1998).
38. B. S. Ham and P. R. Hemmer, "Coherence switching in a four-level system: quantum switching," Phys. Rev. Lett. **84**, 4080–4083 (2000).
39. H. Schmidt and R. J. Ram, "All-optical wavelength converter and switch based on electromagnetically induced transparency," Appl. Phys. Lett. **76**, 3173–3175 (2000).
40. M. Yan, E. G. Rickey, and Y. Zhu, "Observation of absorptive photon switching by quantum interference," Phys. Rev. A **64**, 041801(R) (2001).
41. Y. Chen, G. Pan, and I. A. Yu, "Transient behaviors of photon switching by quantum interference," Phys. Rev. A **69**, 063801 (2004).
42. H. Wang, D. Goorskey, and M. Xiao, "Controlling light by light with three-level atoms inside an optical cavity," Opt. Lett. **27**, 1354–1356 (2002).
43. A. Dawes, L. Illing, S. M. Clark, and D. J. Gauthier, "All-optical switching in rubidium vapor," Science **308**, 672–674 (2005).
44. H. Kang, G. Hernandez, J. Zhang, and Y. Zhu, "Phase-controlled light switching at low light levels," Phys. Rev. A **73**, 011802(R) (2006).
45. L. Li and G. Huang, "Linear and nonlinear light propagations in a Doppler-broadened medium via electromagnetically induced transparency," Phys. Rev. A **82**, 023809 (2010).
46. J. S. Aitchison, A. M. Weiner, Y. Silberberg, M. K. Oliver, J. L. Jackel, D. E. Leaird, E. M. Vogel, and P. W. E. Smith, "Observation of spatial optical solitons in a nonlinear glass waveguide," Opt. Lett. **15**, 471–473 (1990).
47. G. Fanjoux, J. Michaud, H. Maillotte, and T. Sylvestre, "Slow-light spatial solitons," Phys. Rev. Lett. **100**, 013908 (2008).